WALAILAK JOURNAL

Applied Sciences

http://wjst.wu.ac.th https://doi.org/10.48048/wjst.2021.6551

Synthesis and Characterization of TTIP-Al Films and Fe^{3+}/TTIP-Al Films to be Used in Photocatalytic Oxidation under Visible Light

Ketsara INTAWONG[1], Wipawee DECHAPANYA[2,*] and Siriuma JAWJIT[3]

[1]*Civil and Environmental Engineering, School of Engineering and Technology, Walailak University, Nakhon Si Thammarat 80160, Thailand*
[2]*Excellent Center of Environmental Technology and Energy, School of Engineering and Technology, Walailak University, Nakhon Si Thammarat 80160, Thailand*
[3]*School of Public Health, Walailak University, Nakhon Si Thammarat 80160, Thailand*

([*]Corresponding author's e-mail: kwipawee@wu.ac.th)

Received: 16 March 2019, Revised: 23 September 2019, Accepted: 24 October 2019

Abstract

Currently, pressed-wood industries reuse the chemical solution in the wood conservation step by using a chlorine solution. However, this procedure is potentially harmful to workers due to the enormous amount of chlorine use. This research will offer more environmental and human health-friendly solutions to reuse the chemical solution in the process. In this research, the synthesis and characterization of the TTIP-Al films and the Fe^{3+}/TTIP-Al films used in photocatalytic oxidation under visible light was studied. The synthesized films were used to study the COD and color removal of the chemical solution used in the pressed-wood process. To prepare the films, aluminum sheets were cleaned and anodized to increase the films' pore size and roughness for improving the catalyst stabilization on the aluminum substrates. Titanium isopropoxide (TTIP) was used to prepare the TiO_2-Fe^{3+} solution in the sol-gel and dip-coating method. A total of 6 different catalyst dosages of films were synthesized. The morphology of aluminum sheets and the synthesized films were analyzed using SEM. Results revealed that anodization enhanced the pore size and roughness of the film surfaces. The analysis of XRD indicated that the crystal of Anatase TTIP at 25.5° 2 Theta was observed, in which the higher dosage of TTIP resulted in higher peak intensity. Results from the UV-VIS analysis suggested that absorbed wavelengths for Fe^{3+}/TTIP-Al films shifted to visible light (410 nm) compared to those of TTIP-Al films (380 nm). FT-IR Spectra analysis of the Fe^{3+}/TTIP-Al films showed the group of hydroxyl radicals on the Fe^{3+}/TiO_2 surface. This functional group could affect the efficiency of photocatalytic oxidation. Color and COD removal of the chemical solution in rubberwood pressed using these films in the annular photocatalytic reactor will be studied in the next phase of this work.

Keywords: Codoped Fe^{3+}/TTIP, Catalytic film synthesis, Photocatalytic oxidation, Color degradation, Rubber wood process

Introduction

Titanium dioxide (TiO_2) has proved to be a well-known multifunctional nanoparticle because it is regarded as a non-toxic substance that does not link to cancer or disorders in pregnancy. TiO_2 is extensively used in various industries such as food, pigments, medication, and cosmetics [1,2]. TiO_2 is utilized in a wide range of applications due to its chemical stability, robustness against photocorrosion, recyclability, low cost, low solubility, and high reactivity. However, a number of practical problems arise from the use of TiO_2 because of its particle in the form of powder. The past studies regarding the use of TiO_2 as a photocatalyst in photocatalytic oxidation for organic dyes removal have suggested that the main drawback of TiO_2 is the post-separation difficulties associated with its powder form. Additionally, the suspended particles tend to aggregate, resulting in the low efficiency of organic dyes removal. To overcome these difficulties, the immobilization of TiO_2 should be done on supporting materials such as thin films or nanofilms. Moreover, the width of the energy gap of TiO_2 seems to be another problem when TiO_2 is utilized as a photocatalyst. In photocatalytic oxidation, ultraviolet (UV) is one of the major factors that activate a catalyst. Because TiO_2 has a large bandgap of 3.2 eV, a UV light ($\lambda \leq 400$ nm) is required to correspond to the gap. Previous studies have suggested a reduction in the TiO_2 energy gap by doping metal ions to enhance visible-light photocatalytic efficiency. For example, Synthesized Fe^{3+}/TiO_2 and N/TiO_2 thin films coated on stainless steel substrates to be used in photocatalytic oxidation in order to degrade methylene blue and destroy E. Coli under the different ranges of visible light. The study's finding indicated that a 0.5 % Fe^{3+}/TiO_2 film obtained 78.9 % of methylene blue at an initial concentration of 10 - 6 mol under fluorescence, while the degradation of E.Coli under fluorescence at 3 h was 87 % [3]. Therefore, this work focused on synthesizing TiO_2 thin films together with the application of Fe doping. In this study, 6 different catalyst dosages of films were synthesized, including 5, 10, 15 mL TTIP-Al film, 5 % mol Fe^{3+}5 mL Fe^{3+}/TTIP-Al film, 5 % mol. Fe^{3+} 10 mL Fe^{3+}/TTIP-Al film, and 5 % mol Fe^{3+} 15 mL Fe^{3+}/TTIP-Al film. The study's scopes also included an examination of the physical and chemical properties of the synthesized films, their optimization under the visible light, and the use of the films in photocatalytic oxidation to treat wastewater air pollution [4].

Materials and methods

Preparation of aluminum sheets

Aluminum sheets with the size of 25×35×0.002 mm^3 were used as a substrate in this study. The aluminum sheets had been cleaned with 1 M NaOH solution before they were washed with distilled water. In order to increase the pore size for improving the catalyst stabilization on the aluminum substrates, the anodization method was then applied [5]. The anodization was carried out using 18 M H_2SO_4 solution as an electrolyte at a constant applied voltage of 50 V and 0.2 A for 25 min. The anodized films were then washed with distilled water using the ultrasonic cleaner (Model VGT-1012S/GT SONIC) for 15 min before being soaked in acetone for 10 min. After that, the films were washed with distilled water and dried in an oven at 60 °C for 30 min [6]. The process of anodization is illustrated in **Figure 1**.

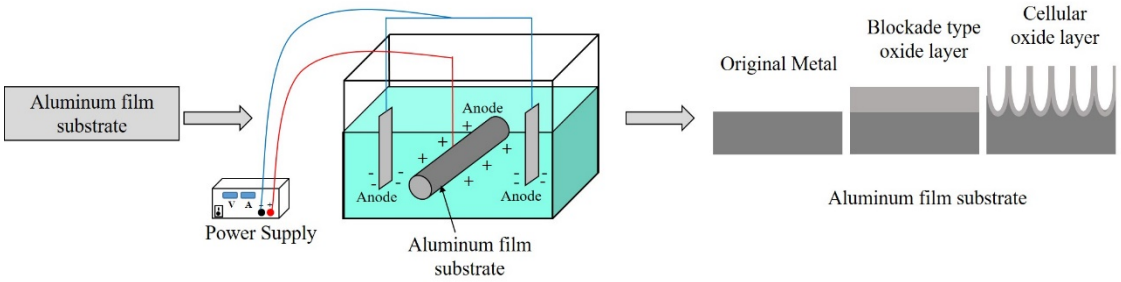

Figure 1 Anodization of aluminum sheets.

Synthesis of TTIP solution and Fe^{3+}/TTIP solution by sol-gel method

TTIP solutions were prepared at 3 different TTIP dosages: 5, 10 and 15 mL. At 5 mL TTIP dosage, 5 mL of titanium (IV) isopropoxide (TTIP) was used as a precursor and dissolved in 90 mL of ethanol. The mixture was stirred for 15 min before being mixed with 125 mL of distilled water. The pH of the system was adjusted to 2 using 2 M hydrochloric acid (HCL). The solution was stirred at 8,000 rpm for 1 h at room temperature and then refluxed by an autoclave at 121 °C for 2 h [7].

Similar to TTIP solutions, Fe^{3+}/TTIP solutions were prepared at 3 different TTIP dosages: 5, 10 and 15 mL. At 5 mL TTIP dosage, 2 sets of solution were prepared: Solution A and solution B. To prepare the solution A, 5 mL of titanium (IV) isopropoxide (TTIP) was used as a precursor and dissolved in 45 mL of ethanol. To prepare the solution B, 228 mg of ferric chloride hexahydrate ($FeCl_3.6H_2O$) at 5 % mol ratio was dissolved in 45 mL of ethanol [8]. The solution A and the solution B were then mixed and stirred for 15 min before being mixed with 125 mL of distilled water. The pH of the system was adjusted to 2 using 2 M hydrochloric acid (HCL). The solution was stirred at 8000 rpm for 1 h at room temperature and then refluxed by an autoclave at 121 °C for 2 h. Fe^{3+}/TTIP solution was obtained.

Dip coating of TTIP-Al films and Fe^{3+}/TTIP-Al films

Anodized aluminum sheets were dipped in the TTIP and Fe^{3+}/TTIP gel solution for 5 times and then dried at room temperature [3]. The films were then dried in a hot air oven at 60 °C for 30 min and calcined at 100 °C for 1 h. Finally, the TTIP-Al films and Fe^{3+}/TTIP-Al films were obtained as shown in **Figure 2**.

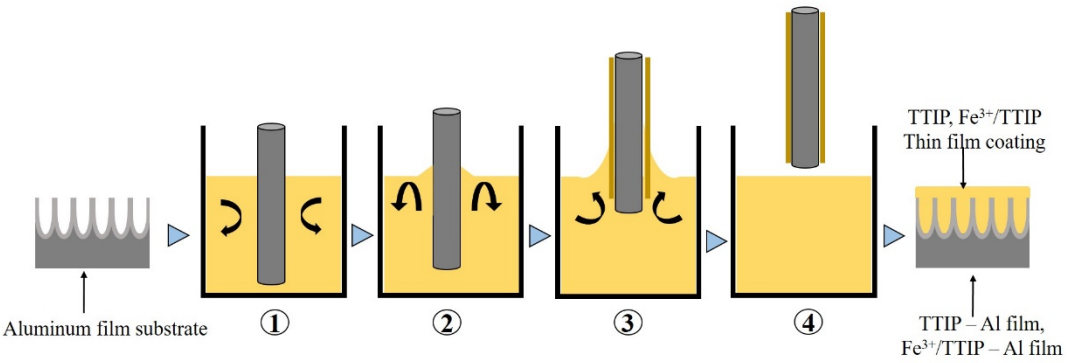

Figure 2 Dip coating of TTIP-Al films and Fe^{3+}/TTIP-Al films

Characterization

The morphology and thickness of the synthesized films were examined using a scanning electron microscope (SEM). The films' particle size distribution was analyzed using the X-ray mapping in SEM (Model Merlin compact, Zeiss).

Energy-dispersive X-ray spectroscopy (EDS) (Model X-MaxN, Oxford Instrument), a microanalytical technique used in conjunction with SEM, was utilized to examine the presence of elements in the synthesized films. The surface area of the films was analyzed in square micrometers (μm2). The spectrum of EDS contains both semi-qualitative and semi-quantitative information.

The crystal structure of TTIP powder and Fe^{3+}/TTIP powder was determined by the X-ray diffraction (XRD) analysis (X-ray Diffract meter; Empyrean, Analytical, Netherlands).

Fourier-transform infrared spectroscopy (FT-IR) is a well-established technique to examine functional groups in organic molecules based on their vibration modes at infrared wavenumbers ranging from 550 - 4,000 cm^{-1}. The spectrometer (Model Tensor 27, Bruker) analyzed functional groups of the synthesized films using the Attenuated Total Reflectance (ATR) technique with ZnSe as a window cell.

Ultraviolet-visible spectrophotometry (UV-VIS) (Jasco V-770 UV-Vis Spectrophotometer) was employed to measure TTIP powder's absorbance Fe^{3+}/TTIP powder in order to calculate their bandgap energy.

The specific surface area of aluminum sheets, anodized aluminum sheets, TTIP-Al films, and Fe^{3+}/TTIP-Al films was analyzed using the Brunauer-Emmett-Teller (BET) technique (Surface Area and Porosity Analyzer (BET), ASAP2460, Micromeritics, USA).

Photocatalytic reactor design

The photocatalytic oxidation reactor used in this study was an annular cylindrical reactor with a total volume of 2.5 L, as shown in **Figure 3**. The photoreactor's outside consisted of an LED-UV light panel that can adjust the light intensity from 0 - 60 watts corresponding to a wavelength range from 400 - 800 nm. TTIP-Al films and Fe^{3+}/TTIP-Al films were placed in the middle of the reactor. To study the color and COD removal of chemical solution, the pump was connected with a chemical solution tank, allowing the solution to flow into the reactor with a flow rate of 10 - 30 LPH [9-13]. The reactor was designed based on an expanded scale in order to be applied in the preservative process in dried rubberwood industries in the south of Thailand.

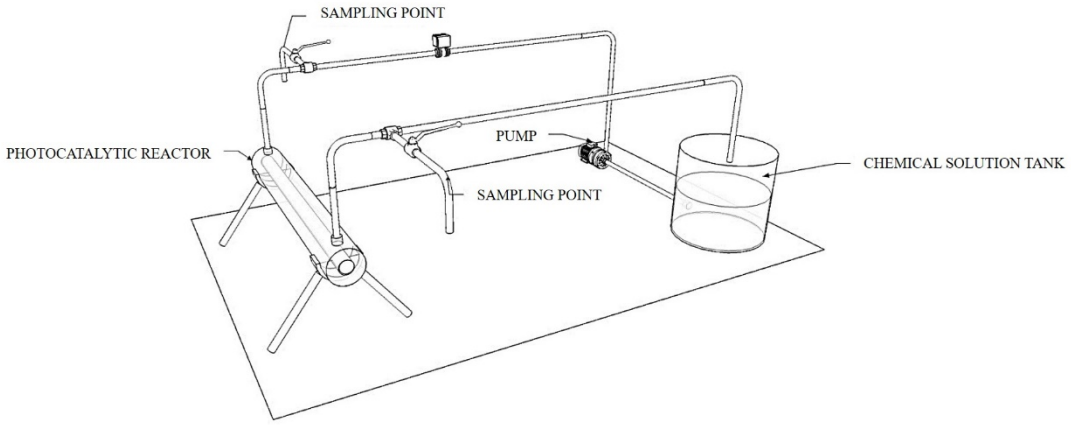

Figure 3 Annular photocatalytic reactor.

Results and discussion

The result of SEM analysis showed that anodization clearly enhanced the pore size of the film surfaces corresponding to pore size analysis from BET. Pore sizes with a diameter ranging from 19.77 - 45.84 nm were found on the anodized aluminum films. This finding is in good agreement with previous works [5,14]. The SEM images of anodized aluminum sheets are shown in **Figure 4**.

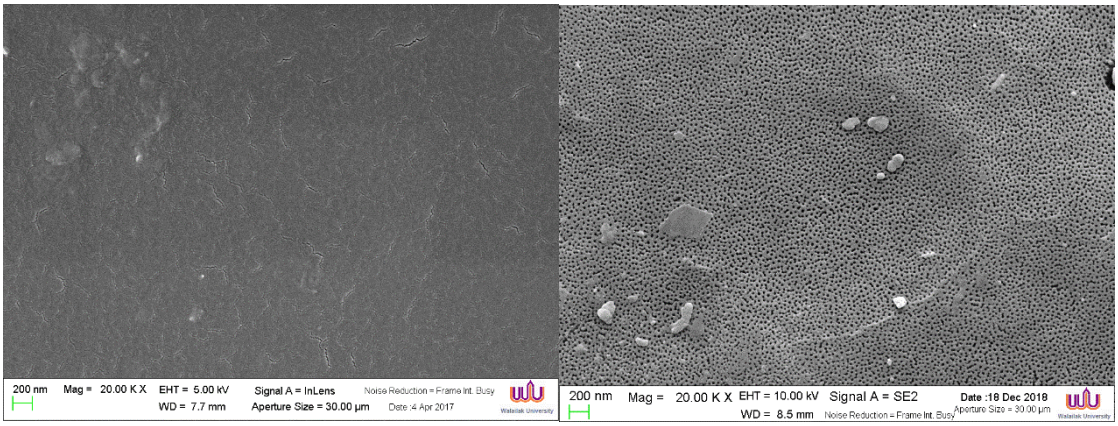

(a) (b)

Figure 4 SEM images of (a) aluminum films 20,000X and (b) anodized aluminum films 20,000X.

Regarding the films' surface analysis, the thickness of catalysts on aluminum film surfaces was 1.30, 2.59, and 3.08 µm for 5, 10, and 15 mL TTIP-Al films, respectively. Meanwhile, the thickness of co-doped catalysts (Fe^{3+}/TTIP-Al films) was slightly lower than those of TTIP-Al films (0.98, 1.26, and 3.02 µm, respectively) because it was clearly seen that colloidal of catalyst in gel solution of TTIP was bigger than that of co-dope catalyst. **Table 1** illustrates the SEM analysis results regarding the thickness of TTIP-Al films and Fe^{3+}/TTIP films.

Table 1 Thickness of TTIP-Al films and Fe^{3+}/TTIP films.

Films	Catalyst Thickness (µm)
5 mL TTIP	1.30
10 mL TTIP	2.59
15 mL TTIP	3.08
5 % mol Fe^{3+}5 mL Fe^{3+}/TTIP	0.98
5 % mol Fe^{3+}10 mL Fe^{3+}/TTIP	1.26
5 % mol Fe^{3+}15 mL Fe^{3+}/TTIP	3.02

In terms of roughness, TTIP-Al films' surface was much rougher than that of Fe^{3+}/TTIP-Al films, which corresponds with previous work [15]. This could be explained that the TTIP solution was clouded by turbidity and contained a number of nanoparticles suspended in the liquid. When the aluminum films were coated with the solution, the surface of the films became rough. On the other hand, the Fe^{3+}/TTIP solution contained fewer nanoparticles. The surface of the films was smoother than those of TTIP-Al films. This finding was similar to previous work [3]. The SEM images of TTIP-Al films and Fe^{3+}/TTIP-Al films are shown in **Figure 5**. From SEM images, TTIP's distribution on Al films was more uniform across the surface for 5 mL of TTIP (compared with 10 and 15 mL TTIP). At a higher dosage of TTIP, the clumps of the catalyst tend to be found on the film surface. This was due to the higher suspension of catalyst existence at higher TTIP concentration. SEM image comparison between TTIP and Fe^{3+}/TTIP suggested that the surfaces of films with co-doped catalyst were smoother because the catalyst suspension in the gel-solution of co-doped catalyst was less than bared TTIP. Results from SEM analysis also

indicated that the particle sizes of 5, 10, 15 mL of TTIP-Al films were in the range of 20 - 600 nm, while the particle sizes of Fe^{3+}/TTIP-Al films cannot be measured because the film surface was too smooth.

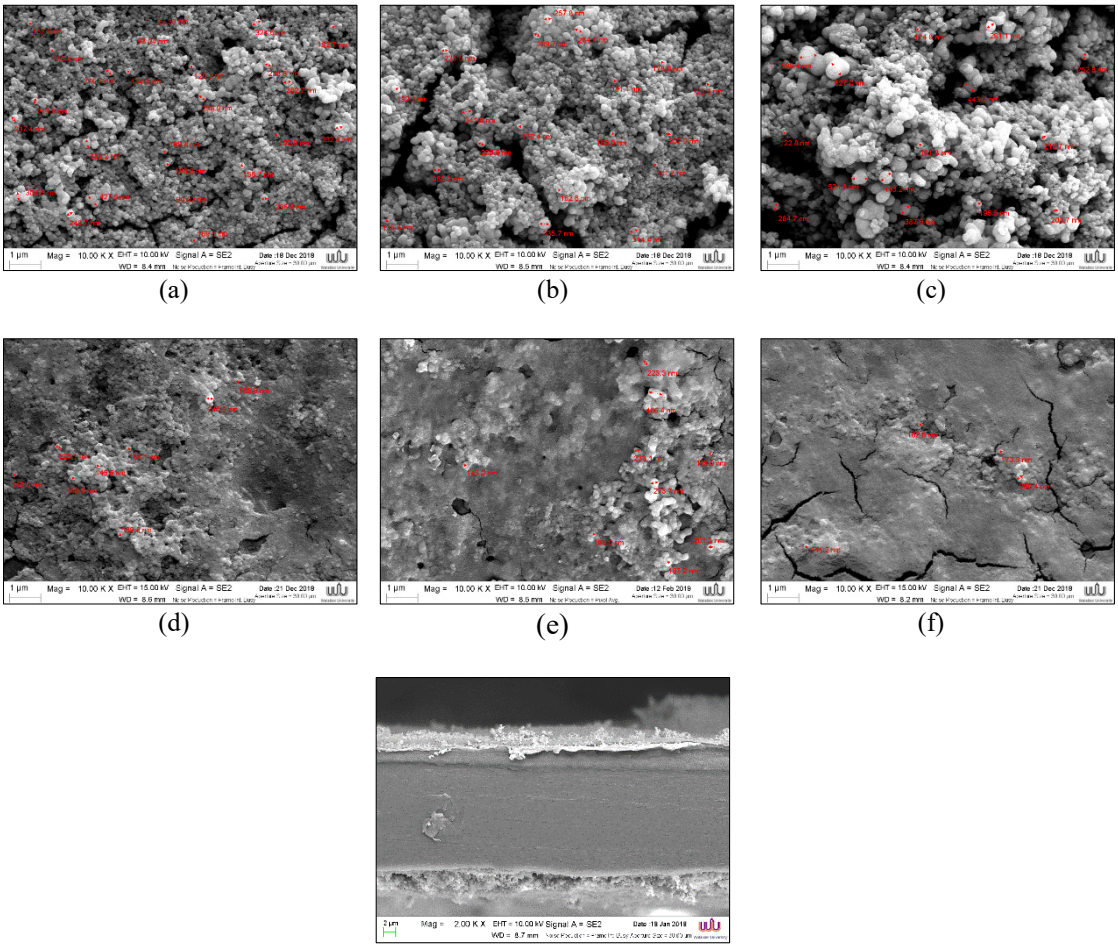

Figure 5 SEM images (10 kV) of (a) 5 mL TTIP-Al film, (b) 10 mL TTIP-Al film, (c) 15 mL TTIP-Al film (d) 5 % mol Fe^{3+} 5 mL Fe^{3+}/TTIP-Al film, (e) 5 % mol Fe^{3+} 10 mL Fe^{3+}/TTIP-Al film (f) 5 % molar Fe^{3+} 15 mL Fe^{3+}/TTIP-Al film and (g) cross-section of 15 mL TTIP-Al film.

Figure 6 illustrates the presence of elemental composition of the synthesized films based on the energy-dispersive X-ray spectroscopy (EDS) analysis. It can be seen that the aluminum films consisted of Al, O, C, and S were allocated to 44.3, 43.2, 8.1, and 4.4 %, respectively. TTIP-Al films at 5, 10, and 15 mL of TTIP dosages contained Ti at 28.4, 38.4, and 48.5 %, respectively. Regarding 5 % mol ratio Fe^{3+}/TTIP-All films at 5, 10 and 15 mL of catalyst dosages, the elements presenting in the films were Ti (16.5, 33.4 and 47.2 %, respectively) and Fe (0.5, 1.2 and 1.8 %, respectively) [16]. As shown in **Figure 6**, the presence of elements in the films is positively correlated with the film layers' thickness. This means the fewer elements result in the films with thinner layers.

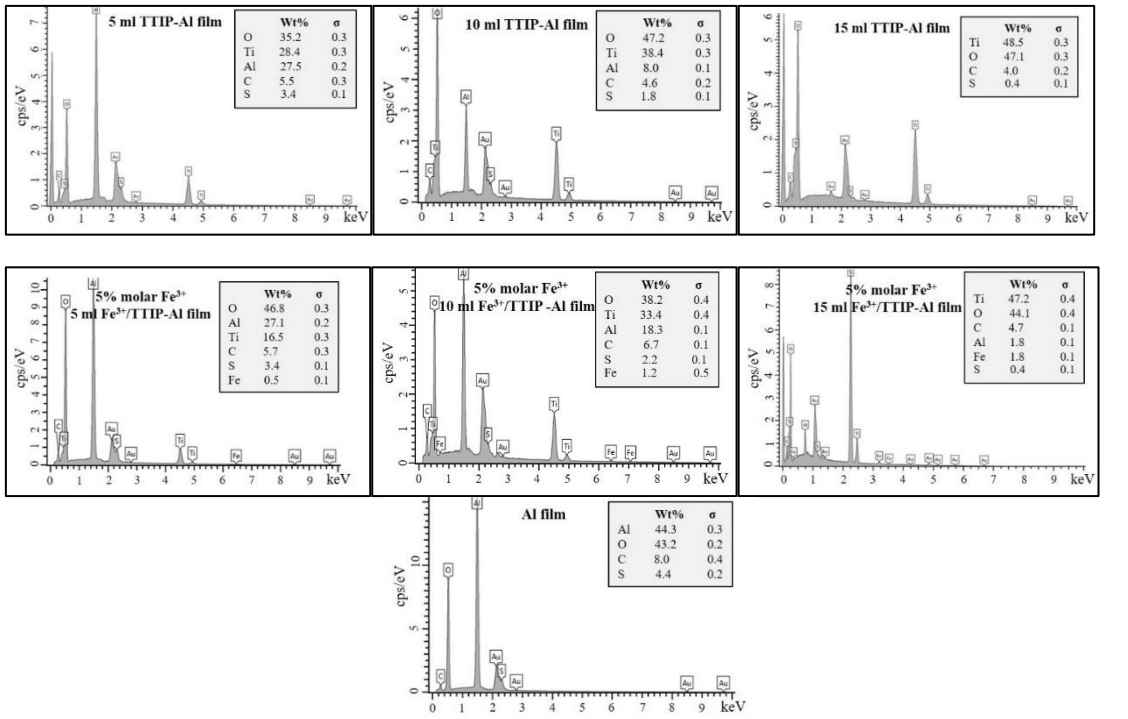

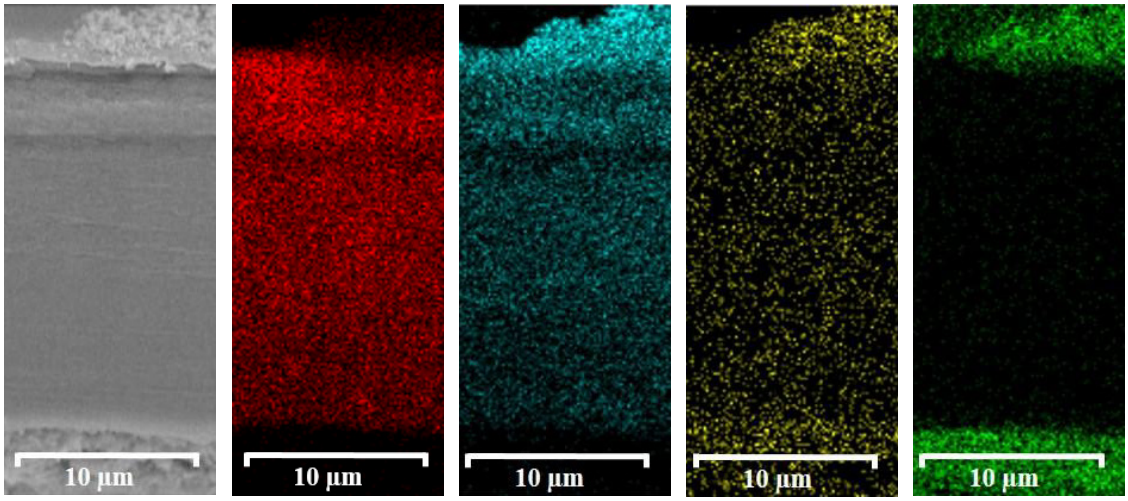

Cross-section TTIP15 mL | C | O | Al | Ti

Figure 6 EDS micrographs of Al film, TTIP-Al films and 5 % mol Fe^{3+}/TTIP-Al films at dosages of 5, 10, 15 mL of TTIP and cross-section of 15 mL TTIP-Al film.

According to the X-ray diffraction (XRD) analysis, as shown in **Figure 7**, anatase peaks were clearly observed at 25.2, 37.7, 47.7, and 54.4° [17], while a peak of brookite was a little bit observed at 30.84°. However, no luminescence of iron oxide (Fe^2O_3) could be observed. This means the mixture of Fe did not significantly affect the change of TiO_2 structure [18]. The peak at 2-theta (degree) and the line broadening at half the maximum intensity (FWHM) were used to calculate the crystal size of TTIP and Fe^{3+}/TTIP powder using the Scherrer equation [19]. The crystal size of TTIP and Fe^{3+}/TTIP was 7.4 and 8.2 nm, respectively [8]. As shown in **Figure 7**, the peak at 2-theta (degree) of TTIP was high in the anatase phrase at 25.2°. With Fe doping, however, the graph with a lower peak and wider base was observed. This is because larger particle sizes increase difficulty in crystallization [16]. Data in **Table 2** show that the increased amount of co-doped catalysts did not significantly influence the crystallized size of the synthesized catalysts. The increasing amount of co-doped catalysts 3 times (5 to 15 mL TTIP) resulted in only a 2.91 % difference in crystallized size.

Table 2 Crystallized Size of TTIP and Fe^{3+}/TTIP sample.

Films	Crytallized Size (nm)
5 mL TTIP	7.56
10 mL TTIP	7.47
15 mL TTIP	7.34
5 % mol Fe^{3+}5 mL Fe^{3+}/TTIP	8.58
5 % mol Fe^{3+}10 mL Fe^{3+}/TTIP	8.36
5 % mol Fe^{3+}15 mL Fe^{3+}/TTIP	7.73

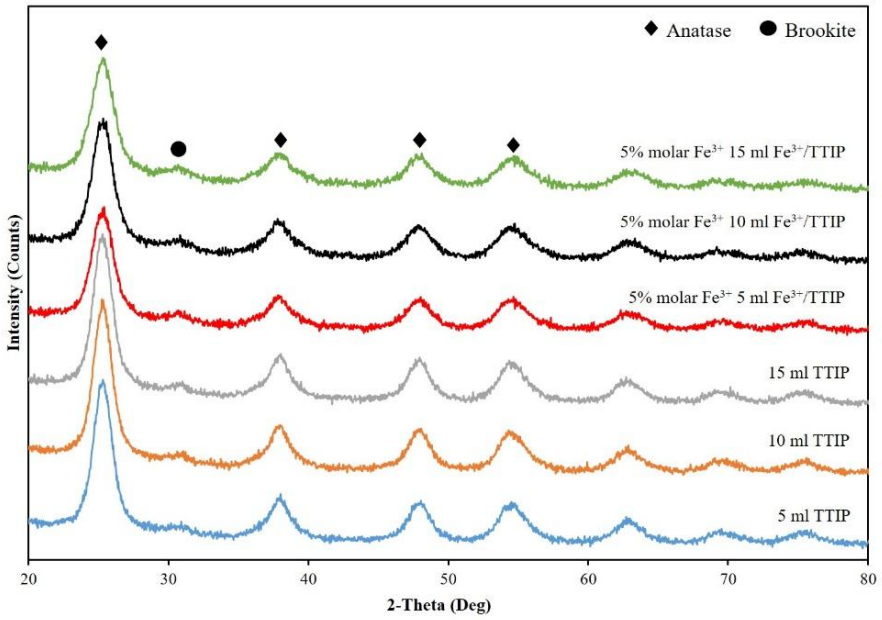

Figure 7 Crystal Identification of TTIP and Fe^{3+}/TTIP using XRD.

The analysis of the chemical functional group of TTIP and Fe^{3+}/TTIP powder was performed using Attenuated Total Reflectance-Fourier Transform Infrared (ATR-FTIR). As shown in **Figure 8**, the wavenumber of 3,400 cm^{-1} is a peak of O-H stretching, which corresponds to the O-H vibration of Ti-OH groups and H2O molecules. The peak of O-H bending, Ti-O stretching, and Fe-O-Ti group is presented at the wave number 1,600, 880 - 450 and 570 cm^{-1}, respectively [4,20,21].

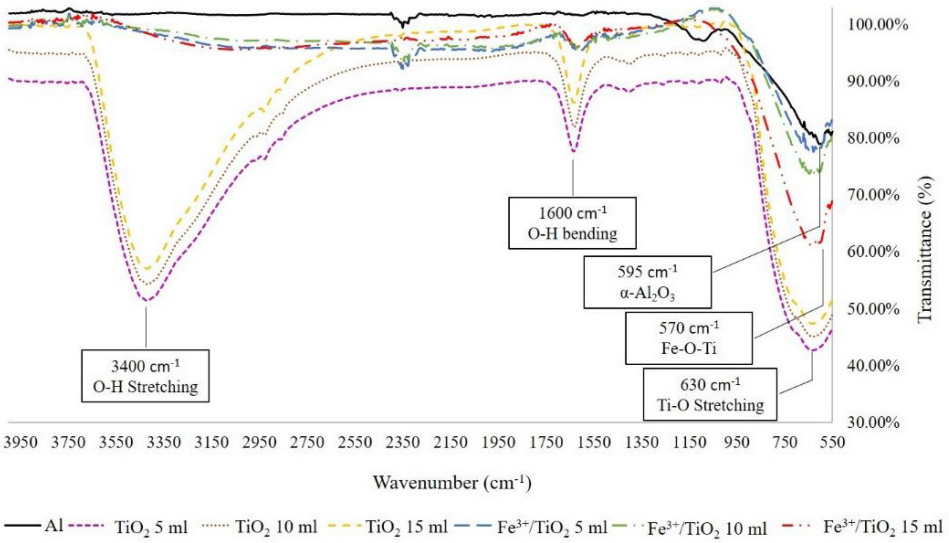

Figure 8 FTIR analysis of Al films, TTIP-Al films and 5 % mol Fe^{3+}/TTIP-Al films at 5, 10, 15 mL dosages of TTIP.

The absorbance of TTIP and Fe^{3+}/TTIP powder was measured using a UV-Visible spectrophotometer, as shown in **Figure 9**. BaSO4 was used as a reference of the TiO_2 energy band to draw a tangent to the inflection point on the curve of spectra before calculating the bandgap energy [22]. **Table 3** illustrates the absorbed wavelengths of TTIP and Fe^{3+}/TTIP powders as well as the bandgap energy (Eg) calculated from absorption edge wavelength (λae) using Max Planck's equation. The wavelength of bare-TiO_2 was at 380 nm (in UV ranges), but the wavelength of co-doped Fe^{3+}/TTIP was 420 nm (invisible ranges). **Figure 9** also displays the influence of increasing the dosage of TTIP and Fe^{3+}/TTIP powder on the catalytic powder's adsorption edge. It is clearly seen that the adsorption edge of the co-doped Fe^{3+}/TTIP powder comparing with that of TTIP powder is extended greatly toward the visible light with the increasing amount of Fe^{3+} and TTIP. These results are induced by the electron transition from Fe^{3d} orbitals to the TTIP conduction band [23].

Table 3 Absorbed wavelength and band gap energy of TTIP powder and Fe^{3+}/TTIP powder.

Type of powder	Wavelength (nm)	Band gap energy (eV)
5 mL TTIP	380	3.26
10 mL TTIP	385	3.22
15 mL TTIP	387	3.20
5 % mol Fe^{3+}5 mL Fe^{3+}/TTIP	410	3.02
5 % mol Fe^{3+}10 mL Fe^{3+}/TTIP	415	2.98
5 % mol Fe^{3+}15 mL Fe^{3+}/TTIP	420	2.95

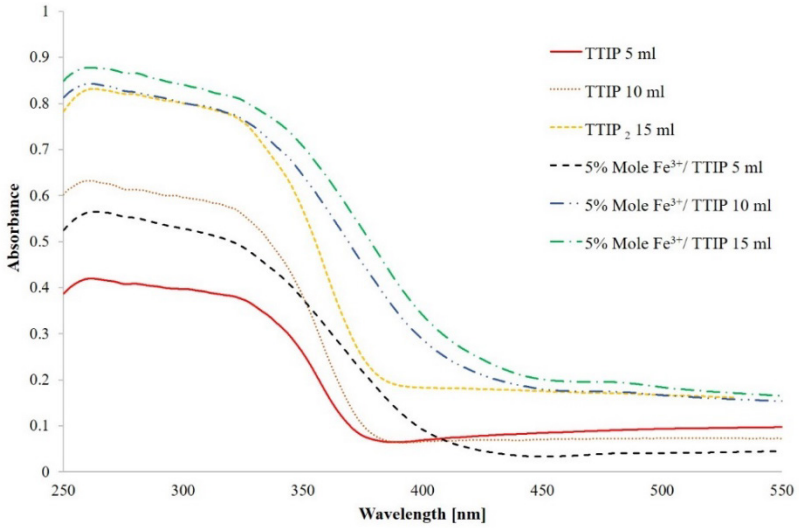

Figure 9 UV-VIS analysis of TTIP and Fe^{3+}/TTIP powder at different concentrations.

Results are displayed in **Figure 10**; as seen from the figure, the specific surface area (SSA) of the anodized Al sheet was the highest. For catalyst doping Al films, the higher dosage of used catalyst resulted in higher SSA and lower pore diameters of the films except for 5 % mol Fe^{3+}15 mL Fe^{3+}/TTIP-Al film. This finding was analogous with the XRD results in which Fe^{3+}/TTIP catalysts had a larger crystallized size than bared TTIP (**Table 2**) SEM images. In other words, this finding revealed that co-dope catalyst-Al films tended to have a smoother surface. Therefore, co-doped catalyst films would obtain higher COD and color removal efficiencies due to photocatalytic oxidation on the films.

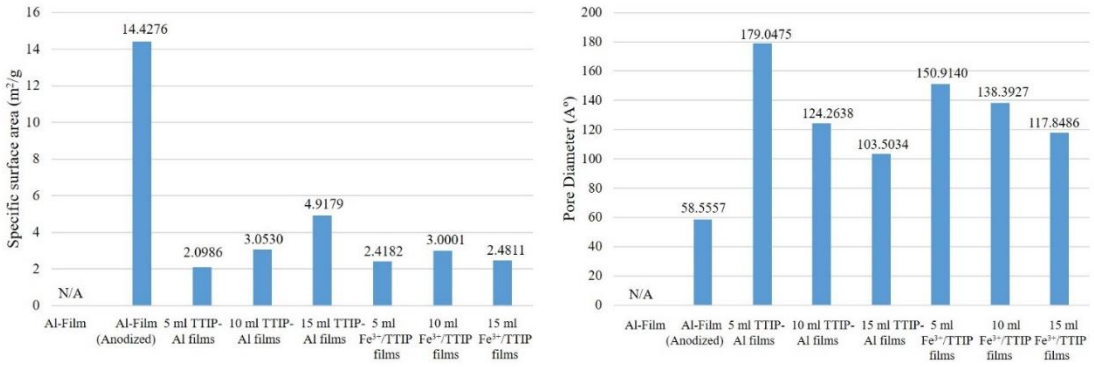

(a) (b)

Figure 10 BET analysis of TTIP-Al films and Fe^{3+}/TTIP-Al films **(**a**)** Specific surface area **(**b**)** Pore Diameter.

Conclusions

In this study, 2 types of films were synthesized: TTIP-Al films and Fe^{3+}/TTIP-Al films. The films were used in a photocatalytic reactor for color degradation of chemical solutions in this study's wood rubber process. The studied parameters included Fe doping and different concentrations of TTIP. Based on the SEM analysis, the thickness of the films was in the range of 0.98 - 3.08 µm. The presence of Ti in the films depends on initial concentrations of TTIP and Fe doping. At low initial concentrations, small amounts of Ti existed in the films. From SEM images, TTIP's distribution on Al films was more uniform across the surface for 5 mL of TTIP (compared with 10 and 15 mL TTIP). At a higher dosage of TTIP, the clumps of the catalyst tended to be found on the film surface. This was due to the higher suspension of catalyst existence at higher TTIP concentration. SEM image comparison between TTIP and Fe^{3+}/TTIP suggested that the surfaces of films with co-doped catalyst were smoother because the catalyst suspension in the gel-solution of co-doped catalyst was less than bared TTIP. This is because the Fe^{3+}/TTIP gel solution was clearer and contained fewer nanoparticles. Additionally, the XRD analysis indicated that TTIP had the anatase-type crystal structure. The crystal size of Fe^{3+}/TTIP-Al films was bigger than that of TTIP-Al films. The FT-IR analysis also revealed the group of hydroxyl radicals on the Fe^{3+}/TiO_2 surface. This functional group could affect the efficiency of photocatalytic oxidation. Moreover, the UV-VIS analysis also showed that Fe doping could reduce the width of the energy band gap of TiO_2 and increase the efficiency of photocatalytic oxidation under visible light.

Acknowledgements

This work was financially supported by Research Grant from Walailak University No.02/2561.

References

[1] JJ Yin, J Liu, M Ehrenshaft, JE Roberts, PP Fu, RP Mason and B Zhao. Phototoxicity of nano titanium dioxides in HaCaT keratinocytes-generation of reactive oxygen species and cell damage. *Toxicol. Appl. Pharmacol*. 2013; **263**, 81-8.

[2] SNA Shah, Z Shah, M Hussain and M Khan. Hazardous effects of titanium dioxide nanoparticles in ecosystem. *Bioinorg. Chem. Appl*. 2017; **2017**, 4101735.

[3] N Muangtrairat, V Rachpech and L Sikong. Photocatalytic and antibacterial properties of TiO_2 composite thin films coated on 304 stainless steel substrate synthesized at sow semperature. *Adv. Mat. Res.* 2011; **214**, 444-9.

[4] Q Wang, S Xu and F Shen. Preparation and characterization of TiO_2 photocatalysts co-doped with iron (III) and lanthanum for the degradation of organic pollutants. *Appl. Surf. Sci.* 2011; **257**, 7671-7.

[5] NM Chelliah, A Saxena, K Sharma, H Singh and MK Surappa. Surface characterization of nanoporous aluminium oxide films synthesized by single-step DC and AC anodization. *Surface Interfac.* 2017; **7**, 139-45.

[6] I Ali, SR Kim, SP Kim and JO Kim. Anodization of bismuth doped TiO_2 nanotubes composite for photocatalytic degradation of phenol in visible light. *Catal. Today* 2017; **282**, 31-7.

[7] SMHA jawad, AA Taha and MM Salim. Synthesis and characterization of pure and Fe doped TiO_2 thin films for antimicrobial activity. *Optik* 2017; **142**, 42-53.

[8] N Nasralla, M Yeganeh, Y Astuti, S Piticharoenphun, N Shahtahmasebi, A Kompany, M Karimipour, BG Mendis, NRJ Poolton and L Siller. Structural and spectroscopic study of Fe-doped TiO_2 nanoparticles prepared by sol-gel method. *Sci. Iran*. 2013; **20**, 1018-22.

[9] ND Banic, BF Abramovic, DV Sojic, JB Krstic, NL Fincur and IP Bockovic. Efficiency of neonicotinoids photocatalytic degradation by using annular slurry reactor. *Chem. Eng. J*. 2016; **286**, 184-90.

[10] Y Zhang, G Shan, F Dong, C Wang and L Zhu. Glass fiber supported BiOI thin-film fixed-bed photocatalytic reactor for water decontamination under solar light irradiation. *J. Environ. Sci.* 2019; **80**, 277-86.

[11] P Esparza, ME Borges and L Diaz. Studies in a fixed-bed photocatalytic reactor system using natural materials for degradation of a dye contaminant in water. *Water Air Soil Pollut*. 2011; **218**, 549-55.
[12] L Rizzo, J Koch, V Belgiorno and MA. Anderson. Removal of methylene blue in a photocatalytic reactor using polymethylmethacrylate supported TiO_2 nanofilm. *Desalination* 2007; **211**, 1-9.
[13] H Zangeneh, AAL Zinatizadeh, M Habibi, M Akia and MH Is. Photocatalytic oxidation of organic dyes and pollutants in wastewater using different modified titanium dioxides: A comparative review. *J. Ind. Eng. Chem*. 2015; **26**, 1-36.
[14] AMA Elnaiem, AM Mebed, WAE Said and MAA Rahim. Porous and mesh alumina formed by anodization of high purity aluminum films at low anodizing voltage. *Thin Solid Films* 2014; **570**, 49-56.
[15] L Gnanasekaran, R Hemamalini and K Ravichandran. Synthesis and characterization of TiO_2 quantum dots for photocatalytic application. *J. Saudi. Chem. Soc.* 2015; **19**, 589-94.
[16] DV Aware. Synthesis and characterization of Fe-doped TiO_2 nanoparticles by modified sol-gel method. *Int. Res. J. Sci. Eng*. 2018; **A3**, 80-4.
[17] KS Saranya, VVT Padil, C Senan, R Pilankatta, K Saranya, B George, S Wacławek and M Cernik. Green synthesis of high temperature stable anatase titanium dioxide nanoparticles using Gum kondagogu: Characterization and solar driven photocatalytic degradation of organic dye. *Nanomater. Basel* 2018; **8**, 1002.
[18] MJV Romero, JG Santaclara, L Oar-arteta, LV Koppen and DY Osadchii, J Gascona and F Kapteijn. Photocatalytic properties of TiO_2 and Fe-doped TiO_2 prepared by metal organic framework-mediated synthesis. *Chem. Eng. J*. 2019; **360**, 75-88.
[19] A Monshi, MR Foroughi and MR Monshi. Modified Scherrer equation to estimate more accurately nano-crystallite size using XRD. *World J. Nano Sci. Eng.* 2012; **2**, 154-60.
[20] DI Anwar and D Mulyadi. Synthesis of Fe-TiO_2 composite as a photocatalyst for degradation of methylene blue. *Proc. Chem.* 2015; **17**, 49-54.
[21] Y Zhao, C Li, X Liu, F Gu, H Jiang, W Shao, L Zhang and Y He. Synthesis and optical properties of TiO_2 nanoparticles. *Mater. Lett*. 2007; **61**, 79-83.
[22] Q Zhang, L Gao and J Guo. Effects of calcination on the photocatalytic properties of nanosized TiO_2 powders prepared by $TiCl_4$ hydrolysis. *Appl. Catal. B Environ*. 2000; **26**, 207-15.
[23] Z Li, W Shen, W He and X Zu. Effect of Fe-doped TiO_2 nanoparticle derived from modified hydrothermal process on the photocatalytic degradation performance on methylene blue. *J. Hazard Mater*. 2008; **155**, 590-94.